High Resolution Spectral Analysis of Pressure Oscillations in Large Segmented Solid Rocket Motors

Kali Prasad KVASN*, Sankaran S and Anuj Nigam

[1]Dy. Manager, GTF&RDF, TO, [2]Chief General Manager,
SMP&ETF, SDSC SHAR, Sriharikota, Tirupati Dt, AP-524124
[3]Student, Department of Aerospace Engineering, Indian Institute of Technology Madras, Chennai, 600036

Abstract

In the present work various methods of Spectral Analysis are analysed and implemented to get high resolution spectrogram results to find frequencies of pressure oscillation varying with time for a Large Segmented Solid Rocket Motor. The analysis was conducted using MATLAB software package R2022a. Validation of the implemented code has been made using a theoretical signal which was generated using MATLAB program to closely resemble the variation in frequency and amplitude to Large segmented solid rocket motor pressure signal data. Pressure Oscillations in Large Segmented Solid Rocket Motors are caused by vortex shedding at frontal thermal protections (inhibitors) and acoustic response upon from impingement of vortices on surfaces like other inhibitors or rocket motor nozzle. This coupling along with change in internal diameter of rocket motor due to fuel-grain burning causes continuous variation in frequency of pressure oscillations in motor. The conventional Fast-Fourier Transform algorithm used in spectral analysis is unable to produce high resolution results to be able to identify this continuous frequency variation in pressure oscillations.

Keywords: *Pressure Oscillations, Spectral Analysis, Solid Rocket Motor, MATLAB*

1. Introduction

Large Segmented Solid Rocket Motors like S200 are known to exhibit Pressure oscillations during flight. These in-turn lead to thrust oscillations which may lead to critical dynamic loads on the structure of the Launch Vehicle. Thus, study of mechanism of pressure oscillation in Large segmented Solid Rocket Motor and ways to mitigate and control it are of significant importance.

These pressure oscillations have been identified to arise due to periodic vortex shedding at the frontal thermal protections (inhibitor) [1]. The role of inhibitor is to restrict the fuel-grain from burning in axial direction. In large segmented solid rocket motors, the fuel-grain burns radially at high rate which after some burn time leads to inhibitors getting exposed into flow as obstruction. This flow obstruction leads to vortex shedding. The magnitude of Pressure oscillations gets amplified if the frequency of vortex shedding is close to frequency of acoustic modes of the duct. Thus, there is a coupling between vortex shedding and acoustics of rocket motor chamber when the shedding frequency matches chamber acoustic mode [1]. The mechanism behind pressure oscillations in large segmented solid rocket motor can be summarised as due to obstruction of flow inhibitors cause periodic vortex shedding, these vortices travel downstream and impinge on other inhibitors or rocket motor nozzle to generate acoustic feedback which in-turn travels upstream to the location of vortex generation and perturbs the shear layer to complete a positive feedback loop. Further as fuel-grain burns radially in large segmented solid rocket motor, this leads to increased chamber volume which reduces mean flow velocity in the chamber. This reduction in mean flow velocity leads to decrease in frequency of vortex shedding to such an extent that it decouples from the chamber acoustic mode. Reference [1] suggested that further change in volume due to fuel grain burning leads to increase in number of vortices shed which in turn causes increases in vortex shedding frequency. Once again it couples with acoustic mode as it comes close to acoustic frequency mode. This coupling-decoupling of vortex shedding and acoustics causes continuous variation of frequency of pressure oscillation in large segmented solid rocket motor with very high amplitude near acoustic modes.

In order to investigate the presence of above-described phenomenon in Large segmented solid rocket motor and further find frequency at each time instant requires high resolution spectral analysis of pressure signal captured during working of solid rocket motor.

2. LITERATURE REVIEW

The Pressure signal obtained from large segmented solid rocket motor is non-stationary as the mean of the signal is changing with time. The oscillations in pressure are about this mean pressure signal. There are many algorithms to find power spectrum from time-domain signal but as the signal is non-stationary and rapidly varying with time, there are very limited algorithms which give accurate frequency-power results.

2.1 SHORT-TIME FOURIER TRANSFORM

Fourier transform is a method to convert time-domain signal into frequency domain information. In Short-Time Fourier Transform, a series of Fourier Transform is applied by windowing the signal by applying time shift t. The window function $w(t' - t)$ centered around t is applied to the signal $X(t')$ to get windowed signal $X(t')w(t' - t)$. Generally, the window function is square signal which gives value of signal $f(t')$ for a time window which is shifted till all the signal is covered. STFT for a signal $X(t')$ can be defined as,

$$Y(t, f) = \int_{-\infty}^{\infty} X\,(t') \cdot w(t' - t) \cdot e^{-2\pi i f t'} dt' \qquad \ldots..(1)$$

Here, $X(t')$ is Input Signal, f is frequency, t is time and $Y(t, f)$ is STFT output for signal.

This can be like wise performed for discrete signals, but the important thing here is to choose the window length which is based on the resolution trade-off [2]. For instance, if the signal has rapidly fluctuating properties, then shorter window is preferred to enable fine temporal resolution however in the case of signal with slowly fluctuating properties larger window is preferred as it gives finer frequency resolution. This trade-off is characteristic feature of STFT and there is no optimal way to choose window length.

The features of window function also affect the results of STFT, as if the window function is having non-zero value through-out then the windowed signal value is non-zero at end points which might give absurd values in frequency domain. This problem can be solved by using windowing function like Hann function which smoothly goes to zero at ends thus making the windowed signal values starting and ending with zeros with smooth increment which reduces any absurdity in frequency domain results.

But even with all the above improvements some of signal characteristics or frequencies go un-noticed due to windowing effect. The windowing effect might cause loss of signal characteristics at the ends of the window as it does not consider previously processed window to report any features of signal that were present at the end of the window [2]. This problem can be solved using constant overlapping window.

Constant overlapping window uses some amount of data from previously processed window alongside the current window. This essentially does two things: one it increases temporal resolution for same length of window and other it improves results by reporting features of signal which might be present at the ends of non-overlapping windows [2].

2.2 WIGLER-VILLE DISTRIBUTION

Wigler-Ville Distribution is Fourier transform of local Auto-correlation function [3]. Local Auto-correlation function reports if any similarity is there between any segments on left and right and how much they overlap in characteristics. It checks the whole signal for all possible segments giving uniform weights to all segments. But to get actual local properties at an instant more importance or weight should be given to local properties or closer segments and less weight for far away segments [4]. Wigler Ville Distribution does not suffer from leakage effects as in STFT due to windowing thus gives better resolution.

$$W(t,f) = \int_{-\infty}^{+\infty} Z\left(t+\frac{\tau}{2}\right) Z^{*}\left(t-\frac{\tau}{2}\right) e^{-2\pi i f\tau} d\tau \qquad \ldots..(2)$$

Here $W(t,f)$ is wigler-ville distribution, Z and Z^{*} are analytical signal and its conjugate. Due to its quadratic nature, it possesses cross terms which lead to interference. A common strategy to reduce impact of interference is to introduce smooth kernel in wigler-ville distribution. This algorithm is called pseudo-Wigler Ville Distribution which uses ambiguity function which gives higher weights to near segments and lower weights to far segments [5]. However, attenuation of cross-terms by means of smoothening kernel leads to increase of time-frequency spread which reduces precision of representation.

2.3 MAXIMUM ENTROPY METHOD

In practice time series data are measured within some finite time interval and analysis assumes data outside this interval to be zero. To reduce error due to this assumption we use weighting functions like Hann functions. Maximum Entropy method provides alternative method for determining power without using this assumption. In principle method provides means of extending sampled data beyond measurement window by taking weighted sum of known data. The weighing function is called prediction error filter which is determined by minimizing the error power output from least mean square fit of measured data to get predicted data. The Method involves maximization of "Entropy" of the system with respect to the power spectrum, subject to constraints imposed by the data! In spectral analysis this application means maximizing entropy of stationary Gaussian process which is given by [6]:

$$H = \int ln\ \left(P(f)\right) \cdot df \qquad \ldots..(3)$$

Where P (f) is the power-spectrum which should be consistent with auto-correlation function.

To maximise the H with respect to P and with further algebraic manipulations the extremised Entropy occurs when power is given by [6]:

$$P(f) = \frac{P_m \cdot \Delta t}{\left|1-\sum_{n=1}^{m} a_{mn}\, e^{-2\pi i f \Delta t}\right|^2} \qquad \ldots..(4)$$

Here $P(f)$ is the power spectrum while P_m is power output by prediction error filter of order m+1 with elements a_{mn} which can be calculated from the matrix equation given below.

$$\begin{bmatrix} R_0 & R_1 & \cdots & R_m \\ R_1 & R_0 & \cdots & R_{m-1} \\ \vdots & \vdots & \ddots & \vdots \\ R_m & R_{m-1} & \cdots & R_0 \end{bmatrix} \begin{bmatrix} 1 \\ -a_1 \\ \vdots \\ -a_m \end{bmatrix} = \begin{bmatrix} P_m \\ 0 \\ \vdots \\ 0 \end{bmatrix}$$

Figure 1: Algebraic Relations governing Auto-correlation coefficients, Prediction error filter coefficients and Error Power output [6].

Here R (k) is the measured value of auto-correlation function which is dependent of a recursive relation involving prediction-error filter as given below.

To calculate auto-correlation coefficients too, prediction error filter coefficients are required which can be determined as shown in the below example for two-order prediction error-filter [6].

$$R_k = \frac{1}{N}\sum_{i=1}^{N-k} x_i \cdot x_{i+k} \qquad \ldots..(5)$$

$$R_k = \sum_{i=1}^{k} R_{k-i} \cdot a_i \qquad \ldots..(6)$$

For instance, consider a two-point prediction filter: $[1\ a_{11}]$

Now the regressive function will scan through data and filter will predict forward terms using its preceding term and least-square fit is performed to get best value of a_{11} which minimizes error P_1 [6]. For the filter to be stable the coefficients a_{ij} should be less than unity and so to satisfy the criterion the forward power output is averaged by power output obtained by operating the filter in reverse direction.

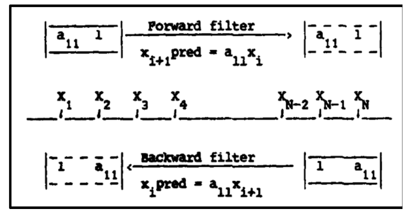

Figure 2: Prediction Error Filter [6]

Thus, by minimizing error with respect to a_{11} we get the following equation shown below [6],

$$a_{11} = \frac{2 \cdot \sum_{i=1}^{N-1} x_i \cdot x_{i+1}}{\sum_{i=1}^{N-1}(x_i{}^2 + x_{i+1}{}^2)} \qquad \ldots..(7)$$

This implementation can be followed for higher number of poles too. Once auto-correlation coefficients are found, power can be calculated.

2.4 *CONTINUOUS WAVELET TRANSFORM*

This Algorithm computes sliding cross-correlation of signal X(t) and family of wavelets as shown below [7]:

$$Y(a,b) = \frac{1}{\sqrt{a}}\int X(t) \cdot \Psi^*\left(\frac{t-b}{a}\right)dt \qquad \ldots..(8)$$

Here a and b are the scales and time shifts of reference wavelet Ψ, Ψ^* is the complex conjugate of reference wavelet. The reference wavelet is also called mother wavelet. Mother wavelets are mean zero oscillatory signals which are given as input by the user. The mother wavelet is cross-correlated with the signal by stretching, dilating and traversing wavelet over it. Thus, longer wavelets are used for low frequencies to improve frequency localization at the cost of temporal localization while for the higher frequencies it works in opposite sense [7]. This algorithm achieves variable time-frequency resolution. Continuous wavelet transform gives wavelet coefficients as output which can be used to plot scalogram [8]. Scalogram is just analogous to spectrogram from short-time Fourier transform.

3. PROBLEM DEFINITION

Target of this study is to achieve very fine (almost continuous; ~0.1Hz/0.1sec) resolution in both frequency and time simultaneously and to be able to observe multiple frequencies modes at any time instant (if available) that might get activated due to fluid-acoustic coupling, find how the frequency clusters/contours vary with time.

4. RESEARCH METHODOLOGY

4.1 *SHORT TIME-FOURIER TRANSFORM*

The hyper-parameters which are critical for high resolution results are choosing length of window as the resolution in time is equal to ratio of length of window and sampling frequency of the signal. But frequency resolution is inverse of that ratio. Thus, larger window gives better frequency resolution but worse time resolution and vice versa. This characteristic of FFT can be exploited by adding zeroes to extend window size, this is called zero-padding and it essentially gives interpolation of frequency data by adding frequency bins due to larger window size without affecting time resolution. But actually, it does not increase resolution in frequency as it is just giving interpolant values.

4.2 *WIGLER-VILLE DISTRIBUTION*

In this Algorithm the signal data was first converted to analytical signal using Hilbert transformation function in MATLAB. Hilbert Transform provides minimum phase-response as the imaginary part of the signal. Further Kernel K(n) was generated by overlaying segments of analytical signal (z) over its conjugate (z*) where n iterates from 1 to N_s (total length of signal) as shown in equation below:

$$k_n(l) = \begin{cases} z(n-l)z^*(n+l), & |l| \leq min\{n, N_s - n\}, \\ 0, & |l| > min\{n, N_s - n\}. \end{cases} \quad \text{.....(9)}$$

$$K(n) = \{\, k_n(-l), \ldots\ k_n(0), \ldots\ k_n(l)\} \quad \ldots..(10)$$

Here l is the length of window which can be taken in exponents of 2 just like FFT. Further FFT was performed over kernel K(n) to get wigler-ville distribution which gives power spectrum. For pseudo-Wigler ville distribution, ambiguity function was taken from MATLAB in-built function to perform wigler-ville distribution algorithm in order to get power spectrum.

4.3 *MAXIMUM ENTROPY METHOD*

In this algorithm, a recursive code is used to find auto-correlation coefficients with equation 5 and 6 as shown in literature review of the algorithm. Further to get error power for every iteration using the algebraic relation shown in figure 2 we can use the following equation [6]:

$$P_m = P_{m-1} \cdot \left(1 - a_{m,m} \cdot {a^*}_{m,m}\right) \quad \ldots..(11)$$

Here m denotes the number of iterations completed and it runs from 1 to M (total length of filter). Error Power output is initialized as [6]:

$$P_0 = \frac{1}{N}\sum_{i=1}^{N} \quad x_i \cdot {x^*}_i \quad \ldots\ldots(12)$$

Here N is total length of signal, x_i and ${x^*}_i$ denote i^{th} element of signal and its conjugate respectively. The length of filter also known as poles in signal processing terms is a hyper-parameter which must be tuned to get finer results. The recursive algorithm calculates filter coefficients and error power for each iteration till it reaches user-input filter length. But selecting filter length is very difficult as too short filter will lead to smoothening of data while too high filter length will lead to splitting of peaks. From various iterations it was found during this study that filter length of 10-25 poles works good for the data encountered in Large segmented solid rocket motor.

4.4 *CONTINUOUS WAVELET TRANSFORM*

In this Algorithm, Mother wavelet is a hyper-parameter which needs to be given as input. The characteristics of mother wavelet affect the resolution of scalogram which is generated from continuous wavelet transform. There are three pre-defined mother wavelets available in MATLAB in-built function to perform continuous wavelet Transform namely Morse wavelet, Mortlet Wavelet and Bump Wavelet. All these wavelets were analyzed in this study.

5. RESULTS AND DISCUSSIONS

Reference Signal was generated to validate all the algorithm implementations as given below:

Table 1: Characteristics of signal

Parameter	Value
Sampling Frequency (f_s)	500 Hz
Time Range	0-140 sec
Signal-to-Noise Ratio	20
Number of Frequency tracks	6

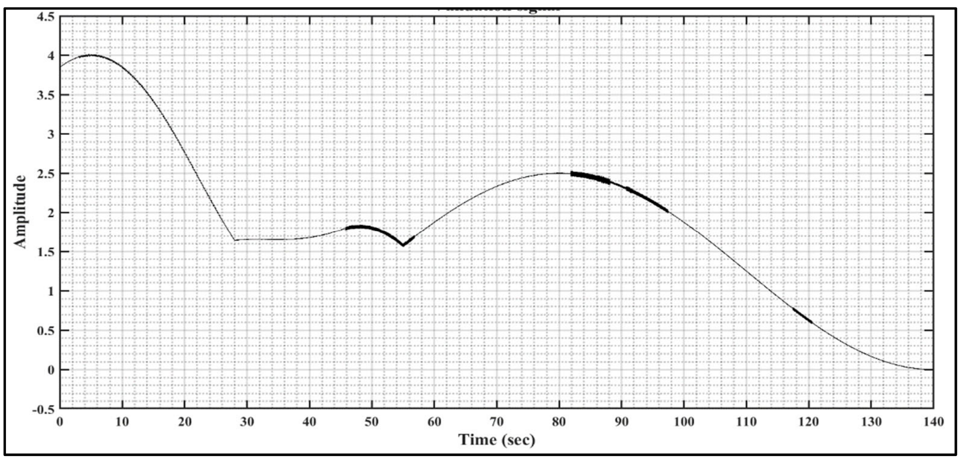

Figure 3 : Reference Signal

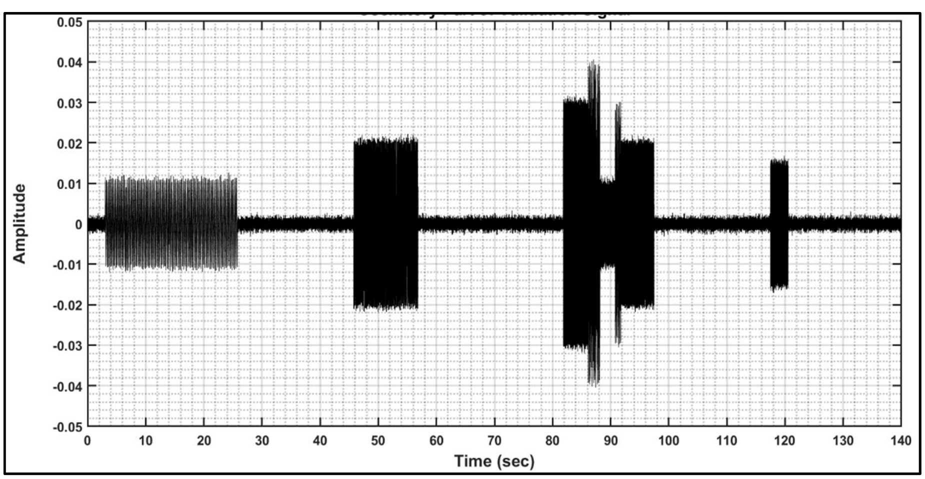

Figure 4: Oscillatory Part of Reference Signal

Mean signal is composed of two Gaussian humps (Hann function) and a quadratic function to mimic solid rocket motor pressure like behavior. Mean signal is superimposed over oscillatory signal which has 6 continuous frequency trains in different time segment to mimic solid rocket motor pressure oscillation behavior.

Table 2: Continuous Frequency tracks

Frequency track (Hz)	Time Range (sec)
5-4.5	3 - 25.8
10-9.5	45.7 - 56.9
32-31	81.8 - 88.2
37-36	86.1 - 91.6
29-30	90.6 - 97.3
65-64	117.3 - 120.4

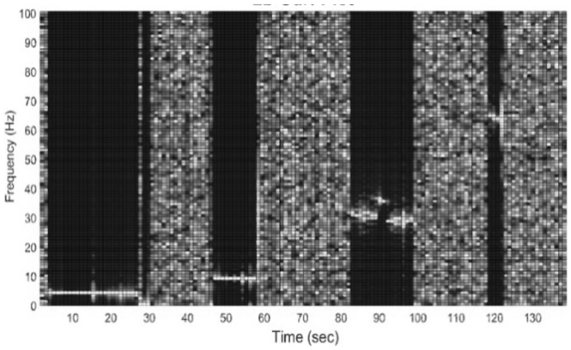

Figure 5: Spectrogram without overlap between windows using STFT

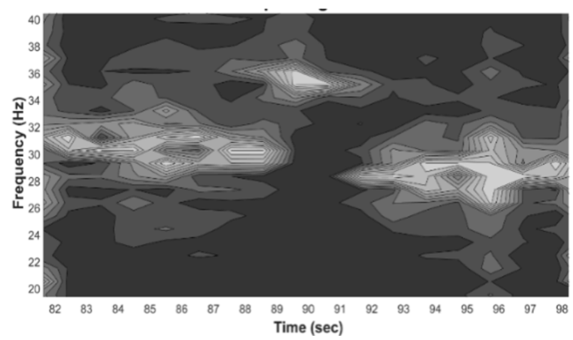

Figure 6: Spectrogram without overlap zoomed to time range of 82 -98 sec

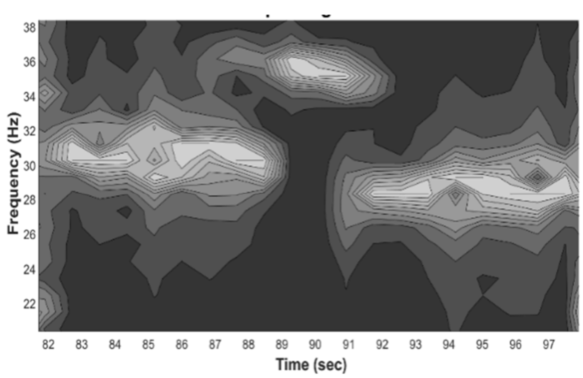

Figure 7: Spectrogram using 20% overlapping window in STFT

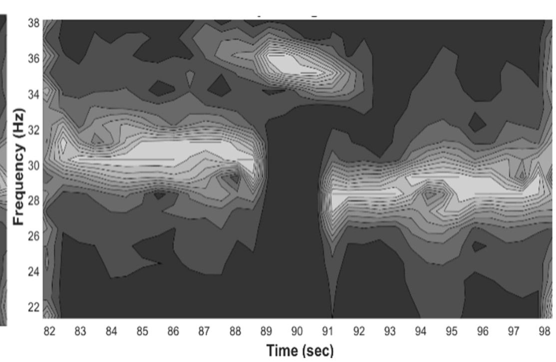

Figure 8: Spectrogram using 50% overlapping window in STFT

It is evident from figure 5 that FFT captures a lot of noise in between frequency tracks. Figure 6 is spectrogram zoomed to time range 82-98 sec as it is region of interest because of three coincident frequency tracks. Further in figure 7 and figure 8 it can be observed that using higher overlapping ratio increases the frequency resolution a bit without affecting much on temporal results. But this increases in resolution is quite low and after 50% overlap the improvement is not visible. Further results from all algorithms will be compared for this region of interest.

ISBN - 978-93-95038-50-8

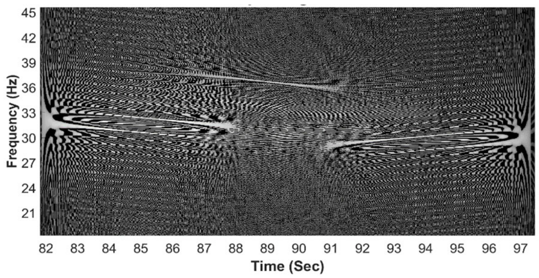

Figure 9: Power Spectrum from Wigler-Ville Distribution

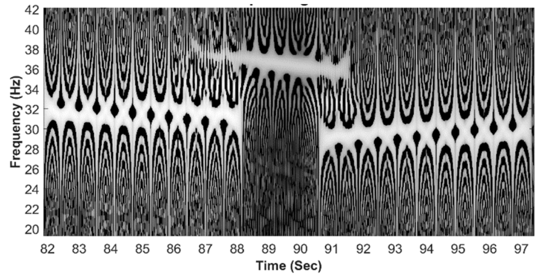

Figure 10: Power Spectrum from Pseudo Wigler-Ville Distribution

From the results of Wigler ville distribution in figure 9 it can be observed that the frequency tracks are highly resolved and overall frequency-time resolution is quite high in the spectrum but a lot of noise is captured in the power spectrum. The pseudo-Wigler ville distribution gives significant reduction in noise but it smoothens out the frequency track making resolution worse.

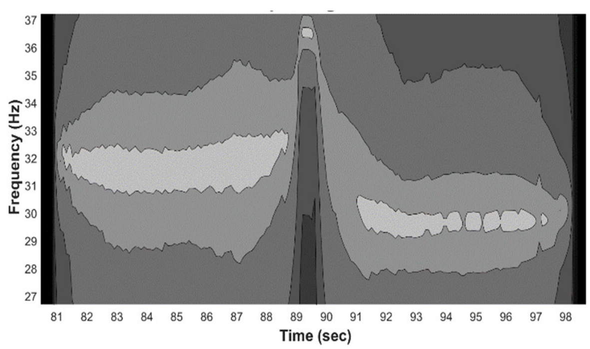

Figure 11: Power Spectrum from Maximum Entropy Method using 10 poles

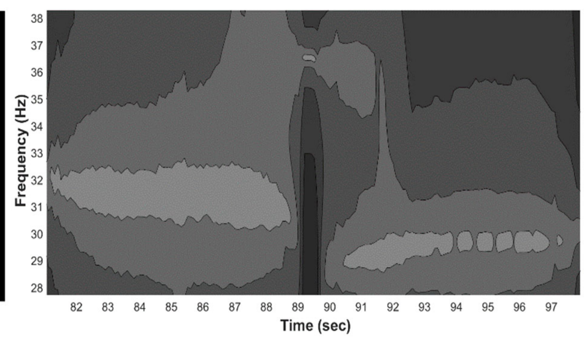

Figure 12: Power Spectrum from Maximum Entropy Method using 20 Poles

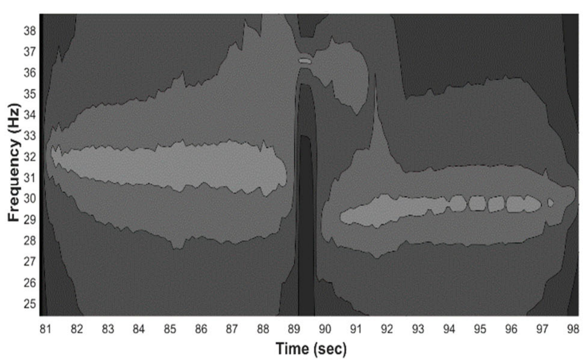

Figure 13: Power Spectrum from Maximum Entropy Method using 25 poles

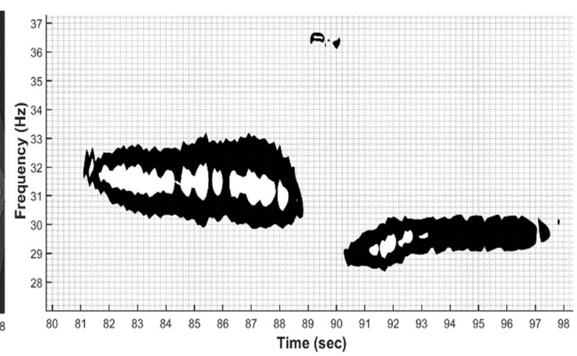

Figure 14: Filtered Power Spectrum from Maximum Entropy Method using 25 poles and filter of 6.3×10^{-4} W/Hz and 2.5×10^{-3} W/Hz

From the results of Maximum Entropy From the results of Maximum Entropy Method, it can be observed at lower poles (10 poles) in figure 11 there is some visible interference between frequency tracks. This interference is reduced as the number of poles increase. After 25 poles the peaks were showing splitting. But with this method there is some interference when frequency tracks coincide. Filtering Power spectrum gives improved results but still some frequency track is lost to interference.

ISBN - 978-93-95038-50-8

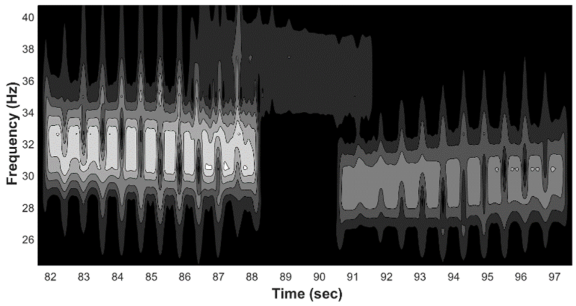

Figure 15: Scalogram from continuous wavelet transform using bump mother wavelet

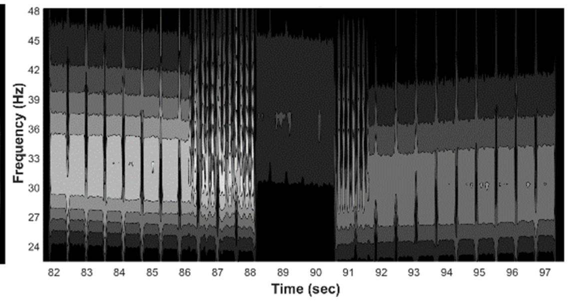

Figure 16: scalogram from continuous wavelet transform using morse mother

Scalogram obtained from Continuous wavelet Transform show high temporal resolution as the frequency tracks precisely start and stop at the time ranges which were used in signal generation as provided in table 2. From all the three wavelets used as mother wavelet, bump wavelet gives best frequency resolution but it is still quite coarse.

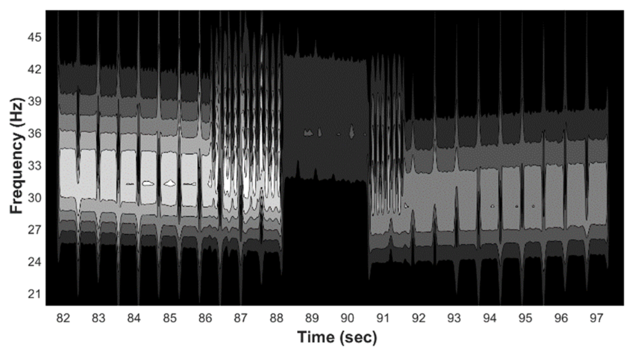

Figure 17: scalogram from continuous wavelet transform using Mortlet mother wavelet

Table 3: Comparision between Algorithms

Algorithms	**Spectral Characteristics**	**Limitations**
Short-Time Fourier transform	Power of signal	Very Coarse resolution
Wigler-Ville Distribution	Frequency and Time (even coincident frequency tracks)	Very high computational space requirement
Maximum entropy Method	Frequency and Time	Interference between coincident frequency tracks
Continuous Wavelet transform	Time	Coarse frequency resolution

6. CONCLUSIONS

From the Results it can be concluded that Wigler-Ville Distribution gives the best resolution in frequency-time but is very computationally heavy algorithm while Maximum Entropy Method also gives fine frequency-time resolution but it shows some interference when frequency tracks are coincident. Hence, Wigler-ville distribution and Maximum Entropy Method are best suitable for analysis of Large Segmented Solid Rocket Motor pressure data. But Wigler-ville can only be performed over small-time interval due to high space requirements. Thus, Maximum Entropy method can be performed over full data, and then if required, small time domain data can be analyzed further with wigler-ville distribution to get finer results.

ISBN - 978-93-95038-50-8

REFERENCES

1. K. Dotson, et.al, Vortex Shedding in a Large Solid Rocket Motor Without Inhibitors at the Segment Interfaces, Journal of Propulsion and Power Vol. 13, No. 2, March – April 1997, https://doi.org/10.2514/2.5170
2. Gröchenig, K. (2001). The Short-Time Fourier Transform. In: Foundations of Time-Frequency Analysis. Applied and Numerical Harmonic Analysis. Birkhäuser, Boston, MA. https://doi.org/10.1007/978-1-4612-0003-1_4
3. O'Toole, J., Mesbah, M., and Boashash, B. (2005). A discrete time and frequency Wigner Ville distribution: Properties and implementation. 8th International Symposium on DSP and Communication Systems, DSPCS'2005, Noosa, Queensland, Australia, 19-21 December 2005.
4. Bradford, Yang, J., & Heaton, T.H. (2005). Variations in the Dynamic Properties of Structures : The Wigner-Ville Distribution by S Case.
5. Y.S. Shin, J.J. Jeon, Pseudo Wigler-Ville Time-Frequency distribution and its applications to machinery condition monitoring, Shock and Vibration, Vol. 1, No. 1, pp. 65-76 (1993) https://doi.org/10.3233/SAV-1993-1109
6. R.W Herring, Maximum Entropy Spectral analysis and Radar signal processing, CRC report Number 1330, January 1980
7. Tary JB, Herrera RH, van der Baan M. 2018 Analysis of time-varying signals using continuous wavelet and synchrosqueezed transforms. Phil. Trans. R.Soc. A 376: 20170254. http://dx.doi.org/10.1098/rsta.2017.0254
8. Sadowsky, J.S. (1994). The continuous wavelet transforms: a tool for signal investigation and understanding.